
Revisiting Contrastive Learning through the Lens of Neighborhood Component Analysis: an Integrated Framework

Ching-Yun Ko
MIT
cyko@mit.edu

Jeet Mohapatra
MIT
jeetmo@mit.edu

Sijia Liu
MSU
liusiji5@msu.edu

Pin-Yu Chen
IBM Research AI
pin-yu.chen@ibm.com

Luca Daniel
MIT
luca@mit.edu

Lily Weng
UCSD
lweng@ucsd.edu

Abstract

As a seminal tool in self-supervised representation learning, contrastive learning has gained unprecedented attention in recent years. In essence, contrastive learning aims to leverage pairs of positive and negative samples for representation learning, which relates to exploiting neighborhood information in a feature space. By investigating the connection between contrastive learning and neighborhood component analysis (NCA), we provide a novel stochastic nearest neighbor viewpoint of contrastive learning and subsequently propose a series of contrastive losses that outperform the existing ones. Under our proposed framework, we show a new methodology to design integrated contrastive losses that could simultaneously achieve good accuracy and robustness on downstream tasks. With the integrated framework, we achieve up to 6% improvement on the standard accuracy and 17% improvement on the adversarial accuracy.

1 Introduction

Contrastive learning has drawn much attention and has become one of the most effective representation learning techniques recently. The contrastive paradigm [1, 2, 3, 4, 5, 6] constructs an objective for embeddings based on an assumed semantic similarity between positive pairs and dissimilarity between negative pairs, which stems from instance-level classification [7, 8, 2]. Specifically, the contrastive loss \mathcal{L}_{CL} [1, 4] is defined as

$$\mathcal{L}_{\text{CL}} := \mathbb{E}_{x \sim \mathcal{D}, x^+ \sim \mathcal{D}_x^+, x_i^- \sim \mathcal{D}_x^-} \left[-\log \frac{e^{f(x)^T f(x^+)}}{e^{f(x)^T f(x^+)} + \sum_{i=1}^N e^{f(x)^T f(x_i^-)}} \right], \quad (1)$$

where, for an input data sample x , (x, x^+) denotes a positive pair and (x, x^-) denotes a negative pair. The function f is parameterized by a neural network and the number of negative pairs N is typically treated as a hyperparameter. Note that the contrastive loss can encode the inputs and keys by different encoders if one considers the use of memory bank or momentum contrast [2, 3, 9]. In this work, we will focus on the paradigm proposed in [10, 11, 4] which has demonstrated impressive results in representation learning.

When constructing loss \mathcal{L}_{CL} in Equation (1), ideally, one draws x^+ from the data distribution \mathcal{D}_x^+ that characterizes the semantically-*similar* (i.e., *positive*) samples to x ; similarly, one wants to draw x^-

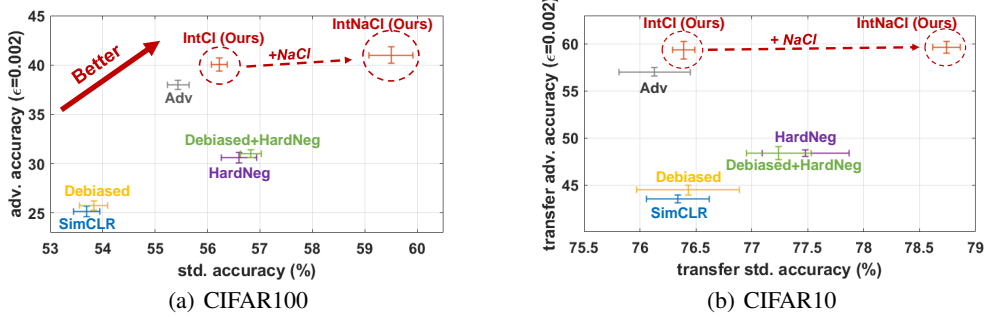


Figure 1: The performance of existing methods and our proposal (IntNaCl & IntCl) in terms of their standard accuracy (x-axis) and adversarial accuracy under FGSM attacks $\epsilon = 0.002$ (y-axis). The transfer performance refers to fine-tuning a linear layer for CIFAR10 with representation networks trained on CIFAR100.

from \mathcal{D}_x^- that characterizes the semantically-dissimilar (*negative*) samples. However, the definition of semantically-similar and semantically-dissimilar is heavily contingent on downstream tasks: an image of a cat can be considered semantically similar to that of a dog if the downstream task is to distinguish between animal and non-animal classes. Without the knowledge of downstream tasks, \mathcal{D}_x^+ and \mathcal{D}_x^- are hard to define. To provide a surrogate of measuring similarity, current mainstream contrastive learning algorithms [3, 4, 9, 6] typically build up \mathcal{D}_x^+ by considering data augmentation $\mathcal{D}_x^{\text{aug}}$ of a data sample x . In the meantime, \mathcal{D}_x^- is approximated by the joint distribution \mathcal{D} or $\mathcal{D}_{\setminus x}^{\text{aug}} := \cup_{x' \in \mathcal{D} \setminus \{x\}} \mathcal{D}_{x'}^{\text{aug}}$, and the resulting contrastive loss is known as $\mathcal{L}_{\text{SimCLR}}$ which was proposed in [4]:

$$\mathcal{L}_{\text{SimCLR}} := \mathbb{E}_{x \sim \mathcal{D}, x^+ \sim \mathcal{D}_x^{\text{aug}}, x_i^- \sim \mathcal{D}_{\setminus x}^{\text{aug}}} \left[-\log \frac{e^{f(x)^T f(x^+)}}{e^{f(x)^T f(x^+)} + \sum_{i=1}^N e^{f(x)^T f(x_i^-)}} \right]. \quad (2)$$

Although this formulation seems to put no assumptions on the downstream task classes, in this paper, with the help of Neighborhood Component Analysis (NCA) [12], we discuss several implicit assumptions made on the class probability prior in the formulation of Equation (2). Specifically, we uncover the relationship between stochastic nearest neighbors and positive pairs in contrastive learning, which then motivates a sequence of augmented contrastive losses that work better under practical computational constraints. Furthermore, representation learning has been evaluated mostly by how they cluster or by a metric such as the standard downstream classification accuracy. However, by inspecting the adversarial accuracy of several existing methods (e.g., Figure 1’s y-axis, the classification accuracy when inputs are corrupted by crafted perturbations), one can see the insufficiency of those methods in addressing robustness. We thus present a general integrated contrastive framework that accounts for *both* the standard accuracy and adversarial cases; this method’s performance remains in the desired upper-right region (circled) as shown in Figure 1. A conceptual illustration of our proposals is given in Figure 2.

We summarize our main contributions as follows:

- We relate contrastive losses with Neighborhood Component Analysis (NCA) and generalize it in the contrastive learning setting, which we dub **NaCl**, Neighborhood analysis Contrastive loss;
- Building on top of NaCl, we proposed a generic framework called Integrated contrastive learning (**IntCl** and **IntNaCl**) where we show that the spectrum of recently-proposed contrastive learning losses [5, 13, 14] can be included as special cases of our framework;
- We provide extensive experiments that demonstrate the effectiveness of **IntNaCl** in improving standard accuracy and adversarial accuracy. Specifically, **IntNaCl** improves upon literature [4, 5, 13, 14] by 3-6% and 4-16% in CIFAR100 standard and adversarial accuracy, and 2-3% and 3-17% in CIFAR10 standard and adversarial accuracy, respectively.

2 Related Work

Contrastive learning. In the early work of [7], authors treat every individual image in a dataset as belonging to its one own class and do multi-class classification tasks under the setting. However, this regime will soon become intractable as we have a large dataset. To cope with this, [2] designs a memory bank for storing seen representations (keys) and utilize noise contrastive estimation [15, 16, 17, 1] for representation comparisons. Then, [3] and [9] further improve upon this by storing keys inferred from a momentum encoder other than the representation encoder for x . Finally, besides the practical tricks introduced in SimCLR [4] (e.g.

stronger data augmentation scheme and projector heads), authors of SimCLR also get rid of the memory bank and instead makes use of other samples from the same batch to form contrastive pairs. [18] considers cluster assignment tasks instead of instance learning and design an online algorithm for learning. Specifically, if we fix the trainable prototypes C to be the data batch and choose code Q to be identity, then the swapped prediction problem reduces to similar forms of Equation (3). [6] argues the possibility of forming contrastive losses without the need for negative examples.

In the rest of this paper, we will focus on the setups of SimCLR and the related follow up work [5, 13, 14] due to computational efficiency. A temperature scaling hyperparameter t is normally used in contrastive learning to tune the radius of the hypersphere that representations lie in. For better readability, without loss of generality, we let $t = 1$ in all equations. We let $g_0(x, \{x_i^-\}_i^N)$ denote the negative term $\frac{1}{N} \sum_{i=1}^N e^{f(x)^T f(x_i^-)}$, where the subscript i identifies the summation index and the superscript N identifies the summation limits. We omit the subscript i when the sample index is one dimensional (e.g. x_i^- has 1-D index, x_{ij}^- has 2-D index). Then $\mathcal{L}_{\text{SimCLR}}$ in Equation (2) can be re-written as

$$\mathcal{L}_{\text{SimCLR}} := \mathbb{E}_{x \sim \mathcal{D}, x^+ \sim \mathcal{D}_x^{\text{aug}}, x_i^- \sim \mathcal{D}_{\setminus x}^{\text{aug}}} \left[-\log \frac{e^{f(x)^T f(x^+)}}{e^{f(x)^T f(x^+)} + N g_0(x, \{x_i^-\}_i^N)} \right]. \quad (3)$$

Designing negative pairs in contrastive learning. Several works [19, 5] have come to the awareness of the sampling bias of negative pairs in Equation 3. Specifically, if the negative samples are sampled from \mathcal{D} , we will receive with $1/K$ probability a positive sample in a K -class classification task with balanced classes, biasing the contrastive loss. [5] proposes a *de-biased* contrastive loss to mitigate the sampling bias by explicitly including the class probability prior on the downstream tasks (e.g., with probability 0.1, a positive sample can be used as x_i^- in CIFAR10), and tune the prior as a hyperparameter. We denote the loss from [5] as $\mathcal{L}_{\text{Debiased}}$ and the full equation is shown below:

$$\mathcal{L}_{\text{Debiased}} := \mathbb{E}_{x \sim \mathcal{D}, x^+, v_j \sim \mathcal{D}_x^{\text{aug}}, u_i \sim \mathcal{D}_{\setminus x}^{\text{aug}}} \left[-\log \frac{e^{f(x)^T f(x^+)}}{e^{f(x)^T f(x^+)} + N g_1(x, \{u_i\}^n, \{v_j\}^m)} \right], \quad (4)$$

where the estimator $g_1(x, \{u_i\}^n, \{v_j\}^m)$ is defined by

$$g_1(x, \{u_i\}^n, \{v_j\}^m) = \max \left\{ \frac{1}{1 - \tau^+} \left(\frac{1}{n} \sum_{i=1}^n e^{f(x)^T f(u_i)} - \tau^+ \right) + \frac{1}{m} \sum_{j=1}^m e^{f(x)^T f(v_j)}, e^{-1/t} \right\}$$

and n and m represents the numbers of sampled points in $\mathcal{D}_{\setminus x}^{\text{aug}}$ and $\mathcal{D}_x^{\text{aug}}$ for the re-weighted negative term, τ^+ is the class probability (one receives a positive point with τ^+ probability when sampling

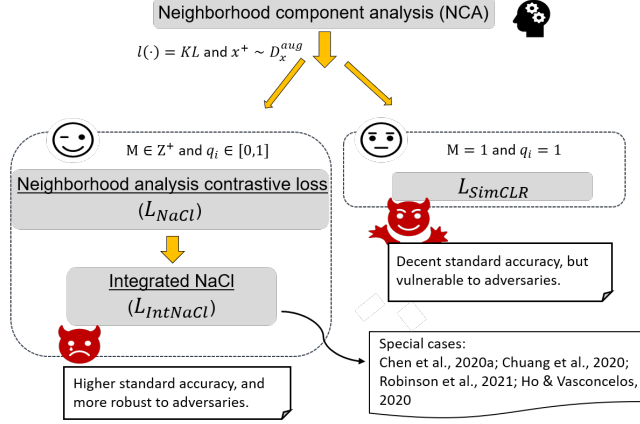


Figure 2: A conceptual illustration of the relationships among NCA, $\mathcal{L}_{\text{SimCLR}}$, and our proposals.

from $\mathcal{D}_{\setminus x}^{\text{aug}}$), and t is the temperature hyperparameter. Recently, [13] proposes to weigh sample pairs through the cosine distance in the estimator $g_1(x, \{u_i\}^n, \{v_j\}^m)$ based on $\mathcal{L}_{\text{Debiased}}$, and we denote their approach as $\mathcal{L}_{\text{Debiased+HardNeg}}$,

$$\mathcal{L}_{\text{Debiased+HardNeg}} := \mathbb{E}_{x \sim \mathcal{D}, x^+ \sim \mathcal{D}_x^{\text{aug}}, v_j \sim \mathcal{D}_{\setminus x}^{\text{aug}}, u_i \sim \mathcal{D}_{\setminus x}^{\text{aug}}} \left[-\log \frac{e^{f(x)^T f(x^+)}}{e^{f(x)^T f(x^+)} + N g_2(x, \{u_i\}^n, \{v_j\}^m)} \right], \quad (5)$$

where the estimator $g_2(x, \{u_i\}^n, \{v_j\}^m)$ is defined by

$$g_2(x, \{u_i\}^n, \{v_j\}^m) = \max \left\{ \frac{1}{1 - \tau^+} \left(\frac{\sum_{i=1}^n e^{(\beta+1)f(x)^T f(u_i)}}{\sum_{i=1}^n e^{\beta f(x)^T f(u_i)}} - \tau^+ \frac{1}{m} \sum_{j=1}^m e^{f(x)^T f(v_j)} \right), e^{-1/t} \right\}$$

A typical choice of n and m are $n = N$ and $m = 1$, and the hyperparameter τ^+ in g_2 is exactly the same as that in g_1 whereas the hyperparameter β controls the weighting mechanism. Specifically, when $\tau^+ = 0$, we denote $\mathcal{L}_{\text{Debiased+HardNeg}}$ as $\mathcal{L}_{\text{HardNeg}}$; when $\beta = 0$, Equation (5) degenerates to Equation (4) which is $\mathcal{L}_{\text{Debiased}}$.

Designing positive pairs in contrastive learning. In parallel to the above line of work, another direction is to augment the construction of positive pairs [14, 20]. Specifically, authors of [14] define the concept of *adversarial examples* in the regime of representation learning as the positive sample that maximizes $\mathcal{L}_{\text{SimCLR}}$ (i.e. Equation (3)) within a pre-specified perturbation magnitude. The resulting loss function is \mathcal{L}_{Adv} :

$$\mathcal{L}_{\text{Adv}} := \mathbb{E}_{x \sim \mathcal{D}, x^+ \sim \mathcal{D}_x^{\text{aug}}, x_{i_1}^- \sim \mathcal{D}_{\setminus x}^{\text{aug}}, x_{i_2}^- \sim \mathcal{D}_{\setminus x}^{\text{adv}}} \left[-\log \frac{e^{f(x)^T f(x^+)}}{e^{f(x)^T f(x^+)} + N g_0(x, \{x_{i_1}^- \}^N)} - \alpha \log \frac{e^{f(x)^T f(x^{\text{adv}})}}{e^{f(x)^T f(x^{\text{adv}})} + N g_0(x, \{x_{i_2}^- \}^N)} \right], \quad (6)$$

where the $\mathcal{D}_{\setminus x}^{\text{adv}}$ is defined by $\cup_{x' \in \mathcal{D} \setminus \{x\}} x' \cup x'^{\text{adv}}$. Notably, one can adjust the importance of the adversarial term by tuning α in Equation (6). A recent work [21] exploits pseudo-label supervision by k-means clustering and performs min-max adversarial training. A relevant idea is exploited by [22] albeit in the supervised learning setting, where the adversarial logit paring works under a supervised learning regime and encourages an adversarial sample x' to have the same logit output as the clean x . In [23], authors construct supervised contrastive loss using multiple positive pairs defined by samples with the same label. Another related work is InfoMin [24], which needs a small amount of labeled data to perform two-step trainings. In the first step, a view generator is learned by minimizing the mutual information between latents from views while ensuring all of them can be correctly classified; in the second step, the trained generator is frozen and the representation network is learned by maximizing the mutual information between latents from views. We note that InfoMin can be regarded as inserting a learned “hard positive sample” into contrastive learning. [25] inherits the usage of a memory bank as in [3] and select from it the representation candidate z' nearest to $z = f(x)$ (determined by nearest neighbor). Eventually the loss is formed by substituting z' for z in Equation (3).

Adversarial Robustness. Despite neural networks’ supremacy in achieving impressive performance, they have been proved vulnerable to human-imperceptible perturbations [26, 27, 28, 29]. In the supervised learning setting, an adversarial perturbation δ is defined to render inconsistent classification result of the input x : $r(x + \delta) \neq r(x)$, where r is a neural network classifier. A stronger adversarial attack means it can find δ with higher success attack rate under the same ϵ -budget ($\|\delta\|_p \leq \epsilon$). One of the most popular and classical attack algorithms is FGSM [26], where with a fixed perturbation magnitude ϵ , FGSM uses the sign of cross entropy gradient to decide between $\delta = \epsilon$ and $\delta = -\epsilon$. Another popular attack method we consider in this paper is PGD [30], which assembles the iterative-FGSM [31] but with additional projection steps.

3 Neighborhood analysis Contrastive loss

In this section, we first establish a connection between the literature on Neighborhood Component Analysis (NCA) [12] and the contrastive learning loss in Section 3.1. Inspired by our result in Section

3.1, we further extend the classic contrastive loss to three variant losses in Section 3.2, which we refer to as **Neighborhood analysis Contrastive loss (NaCl)**. Three NaCl methods handle three aspects of $\mathcal{L}_{\text{SimCLR}}$ individually and are beneficial for learning more powerful representations that can achieve higher downstream task accuracy.

3.1 Stochastic nearest neighbor framework

NCA is a supervised learning algorithm concerned with learning a distance metric that maximizes the performance of nearest neighbour classification. As the set of neighbors for a point can remain unchanged within an area around transformation A , the leave-one-out classification performance can be a piecewise-constant function of A and therefore non-differentiable. To overcome this, the optimization problem is generally given using the concept of stochastic nearest neighbors. In the stochastic nearest neighbor setting, nearest neighbor selection is regarded as a random event, where the probability point x_j is selected as the nearest neighbor for x_i is given as $p(x_j | x_i)$ with

$$p_{ij} = p(x_j | x_i) = \frac{e^{-\|Ax_i - Ax_j\|^2}}{\sum_{k \neq i} e^{-\|Ax_i - Ax_k\|^2}} \propto e^{-\|Ax_i - Ax_j\|^2}, j \neq i.$$

Let c_i denote the label of x_i , in the leave-one-out classification loss, the probability a point is classified correctly is given as $p_i = \sum_{j|c_j=c_i} p_{ij}$, where $\{j | c_j = c_i\}$ defines an index set with which all points x_j belong to the same class as point x_i . The probability x_i 's label is c_i is given as q_i , which is exactly 1¹. Thus the optimization problem can be written as $\min_A \sum_{i=1}^n \ell(q_i, \sum_{j|c_j=c_i} p_{ij})$. This learning objective then naturally maximizes the expected accuracy of a 1-nearest neighbor classifier. Two popular choices for $\ell(\cdot)$ are the total variation distance and the KL divergence. In the seminal paper of [12], the authors showed both losses give similar results. We will focus on the KL divergence loss in this work. For $\ell(\cdot) = \text{KL}$, the relative entropy from p to q is $D_{\text{KL}}(q||p) = \sum_i -q_i \log \frac{p_i}{q_i} = \sum_i -\log p_i$, when $q_i = 1$, and the optimization problem becomes

$$\min_A \sum_{i=1}^n -\log \left(\sum_{j|c_j=c_i} \frac{e^{-\|Ax_i - Ax_j\|^2}}{\sum_{k \neq i} e^{-\|Ax_i - Ax_k\|^2}} \right). \quad (7)$$

With the above formulation, we argue that the contrastive learning loss can be given assuming only positive pairs belong to the same class and the transformation Ax is instead parametrized by a function $\frac{f(x)}{\sqrt{2}} = \frac{h(x)}{\sqrt{2}\|h(x)\|}$, where h is a neural network. Specifically, Equation (7) becomes Equation (9):

$$\min_f \sum_{i=1}^n -\log \left(\frac{\sum_{j=1}^M e^{-\frac{1}{2}\|f(x_i) - f(x_j^+)\|^2}}{\sum_{k \neq i} e^{-\frac{1}{2}\|f(x_i) - f(x_k)\|^2}} \right) \quad (8)$$

$$\xrightarrow{\|f(x)\|=1} \min_f \mathbb{E}_{x \sim \mathcal{D}} \left[-\log \left(\frac{\sum_{j=1}^M e^{f(x)^T f(x_j^+)}}{\sum_{j=1}^M e^{f(x)^T f(x_j^+)} + N g_0(x, \{x_i^-\}^N)} \right) \right]. \quad (9)$$

We give the full derivation from Equation (8) to Equation (9) in the appendix. We note that the contrastive loss in [4] is a special case of Equation (9) with $M = 1$, $x^+ \sim \mathcal{D}_x^{\text{aug}}$, which yields the minimization over the exact form of $\mathcal{L}_{\text{SimCLR}}$ as given in Equation (3),

$$\min_f \mathbb{E}_{x \sim \mathcal{D}, x^+ \sim \mathcal{D}_x^{\text{aug}}, x_i^- \sim \mathcal{D}_x^{\text{aug}}} \left[-\log \left(\frac{e^{f(x)^T f(x^+)}}{e^{f(x)^T f(x^+)} + N g_0(x, \{x_i^-\}^N)} \right) \right].$$

As the computation of the loss grows quadratically with the size of the dataset, the current method [4] works in mini batches and constructs positive/negative pairs in a data batch of size N to estimate the loss. In practice, the expectation over $x^+ \sim \mathcal{D}_x^{\text{aug}}$ is estimated with one sample.

¹For every data point, p and q are defined differently with their supports being the class index. For every sample x , q_i is the ground truth probability of class labels and p_i is the prediction probability. By default, we assume every data

3.2 NCA inspired contrastive loss

Based on the connection we have built in Section 3.1, we discover that the reduction from the NCA formulation to $\mathcal{L}_{\text{SimCLR}}$ requires

1. Estimating the expectation over $\mathcal{D}_x^{\text{aug}}$ by one sample;
2. Assuming the expected relative density of positives in the underlying data distribution is $1/N$;
3. The probability induced by representation network q_i are either 1 or 0.

(I) \mathcal{L}_{VAR} . As the first point is straightforward, one can naively design a loss that has a lowered variance compared to $\mathcal{L}_{\text{SimCLR}}$. That is, originally the expectation over $\mathcal{D}_x^{\text{aug}}$ is estimated with only one sample. Now instead, one simulates M trials of the procedure for every data point in a batch. For each batch of training examples we create M copies of the batch by resampling from the augmented distribution, which yields $\mathcal{L}_{\text{VAR}}(g_0, M)$, given by

$$\mathcal{L}_{\text{VAR}}(g = g_0, M) := \mathbb{E}_{x \sim \mathcal{D}, x_j^+ \sim \mathcal{D}_x^{\text{aug}}, x_j^- \sim \mathcal{D}_{\setminus x}^{\text{aug}}} \left[-\frac{1}{M} \sum_{j=1}^M \log \frac{e^{f(x)^T f(x_j^+)}}{e^{f(x)^T f(x_j^+)} + N g_0(x, \{x_{ij}^-\}_{i=1}^N)} \right].$$

This idea is typically referred to as multiview contrastive learning [32, 33, 34].

(II) $\mathcal{L}_{\text{BIAS}}$. Next we shift our focus to the ‘‘demographic’’ of a point’s neighborhood. Since when relating unsupervised SimCLR to supervised NCA, we view two samples in a positive pair as same-class samples. Therefore, having $\{j \mid c_j = c_i\}$ to contain only one element or equivalently $M = 1$ implies the relative density of positives in the underlying data distribution is $M/N = 1/N$, naturally biasing towards some downstream tasks. In order to determine M , as the expected relative density is task-dependent, we treat the M/N ratio as a hyperparameter similar to the class probabilities τ^+ introduced by [5]. Therefore, we experiment with enlarging the index set $\{j \mid c_j = c_i\}$ to include more than one element or equivalently $M \neq 1$. This leads us to the following objective

$$\mathcal{L}_{\text{BIAS}}(g = g_0, M) := \mathbb{E}_{x \sim \mathcal{D}, x_j^+ \sim \mathcal{D}_x^{\text{aug}}, x_i^- \sim \mathcal{D}_{\setminus x}^{\text{aug}}} \left[-\log \frac{\sum_{j=1}^M e^{f(x)^T f(x_j^+)}}{\sum_{j=1}^M e^{f(x)^T f(x_j^+)} + N g_0(x, \{x_i^-\}_{i=1}^N)} \right].$$

(III) $\mathcal{L}_{\text{MIXUP}}$. Finally, to reduce the reliance on the downstream prior, a practical relaxation can be made by allowing neighborhood samples to agree with each other with probability. This translates into relaxing the specification of $q_i = 1$ and consider a synthetic data point $x' = \lambda x_i + (1-\lambda)y$, $y \sim \mathcal{D}$ that belongs to a synthetic class $c_{\lambda, i}$. Assume the probability x_i ’s label is $c_{\lambda, i}$ is $q_{\lambda, i} = \lambda + (1-\lambda)[c_y = c_i]$, then $q_{\lambda, i}$ should match the probability $p_{\lambda, i} = \sum_{j \mid c_j = c_{\lambda, i}} p_{ij}$, where $\{j \mid c_j = c_{\lambda, i}\}$ is a singleton containing only the index of x' , which yields

$$\begin{aligned} \mathcal{L}_{\text{MIXUP}}(g = g_0, M, \lambda) := & \mathbb{E}_{x \sim \mathcal{D}, x^+ \sim \mathcal{D}_x^{\text{aug}}, x_{i_1}^-, x_{i_2 j}^-, x_j^- \sim \mathcal{D}_{\setminus x}^{\text{aug}}} \left[-\log \frac{e^{f(x)^T f(x^+)}}{e^{f(x)^T f(x^+)} + N g_0(x, \{x_{i_1}^-\}_{i_1}^N)} \right. \\ & - \frac{\lambda}{M-1} \sum_{j=1}^{M-1} \log \frac{e^{f(x)^T f(\lambda x^+ + (1-\lambda)x_j^-)}}{e^{f(x)^T f(\lambda x^+ + (1-\lambda)x_j^-)} + N g_0(x, \{x_{i_2 j}^-\}_{i_2}^N)} \\ & \left. - \frac{1-\lambda}{M-1} \sum_{j=1}^{M-1} \log \left(1 - \frac{e^{f(x)^T f(\lambda x^+ + (1-\lambda)x_j^-)}}{e^{f(x)^T f(\lambda x^+ + (1-\lambda)x_j^-)} + N g_0(x, \{x_{i_2 j}^-\}_{i_2}^N)} \right) \right]. \end{aligned}$$

Interestingly, the construction of x' herein assembles the mixup [35] philosophy in supervised learning. We therefore name this loss by $\mathcal{L}_{\text{MIXUP}}$. Recent work [36, 37] have also considered augment the dataset by including synthetic data point and build domain-agnostic contrastive learning strategies (the formed contrastive loss takes slightly different form). Based on the idea of neighborhood demographics, our intuition of extending to $\mathcal{L}_{\text{MIXUP}}$ also explains [36, 37]’s excellent performance under insufficient domain knowledge well.

Table 1: The relationship between IntNaCl framework and the literature.

$\mathcal{L}_{\text{IntNaCl}}$	$\mathcal{L}_{\text{NaCl}}(g^1, M, \lambda)$				α	$\mathcal{L}_{\text{Robust}}(g^2, w)$	
	$\mathcal{L}_{\text{NaCl}}$	g^1	M	λ		g^2	w
$\mathcal{L}_{\text{SimCLR}}$ [4]	$\mathcal{L}_{\text{VAR}}/\mathcal{L}_{\text{BIAS}}/\mathcal{L}_{\text{MIXUP}}$	g_0	1	-	0	-	-
$\mathcal{L}_{\text{Debiased}}$ [5]	$\mathcal{L}_{\text{VAR}}/\mathcal{L}_{\text{BIAS}}/\mathcal{L}_{\text{MIXUP}}$	g_1	1	-	0	-	-
$\mathcal{L}_{\text{Debiased+HardNeg}}$ [13]	$\mathcal{L}_{\text{VAR}}/\mathcal{L}_{\text{BIAS}}/\mathcal{L}_{\text{MIXUP}}$	g_2	1	-	0	-	-
\mathcal{L}_{Adv} [14]	$\mathcal{L}_{\text{VAR}}/\mathcal{L}_{\text{BIAS}}/\mathcal{L}_{\text{MIXUP}}$	g_0	1	-	1	g_0	1
$\mathcal{L}_{\text{IntCl}}$ in Fig. 1	$\mathcal{L}_{\text{VAR}}/\mathcal{L}_{\text{BIAS}}/\mathcal{L}_{\text{MIXUP}}$	g_2	1	-	1	g_2	$\hat{w}(x)$
$\mathcal{L}_{\text{IntNaCl}}$ in Fig. 1	$\mathcal{L}_{\text{MIXUP}}$	g_2	5	0.5	1	g_2	$\hat{w}(x)$

Table 2: A summary of definitions.

$\mathcal{L}_{\text{VAR}}(g^1, M)$	$\mathbb{E}_{x \sim \mathcal{D}, x_j^+ \sim \mathcal{D}_x^{\text{aug}}, x_j^- \sim \mathcal{D}_{\setminus x}^{\text{aug}}} \left[-\frac{1}{M} \sum_{j=1}^M \log \frac{e^{f(x)^T f(x_j^+)}}{e^{f(x)^T f(x_j^+)} + N g^1(x, \{x_{i_j}^-\}_i^N)} \right]$
$\mathcal{L}_{\text{BIAS}}(g^1, M)$	$\mathbb{E}_{x \sim \mathcal{D}, x_j^+ \sim \mathcal{D}_x^{\text{aug}}, x_i^- \sim \mathcal{D}_{\setminus x}^{\text{aug}}} \left[-\log \frac{\sum_{j=1}^M e^{f(x)^T f(x_j^+)}}{e^{f(x)^T f(x_j^+)} + N g^1(x, \{x_i^-\}_i^N)} \right]$
$\mathcal{L}_{\text{MIXUP}}(g^1, M, \lambda)$	$\mathbb{E}_{x \sim \mathcal{D}, x^+ \sim \mathcal{D}_x^{\text{aug}}, x_{i_1}^-, x_{i_2}^-, x_j^- \sim \mathcal{D}_{\setminus x}^{\text{aug}}} \left[-\log \frac{e^{f(x)^T f(x^+)}}{e^{f(x)^T f(x^+)} + N g^1(x, \{x_{i_1}^-\}_i^N)} \right]$ $-\frac{\lambda}{M-1} \sum_{j=1}^{M-1} \log \frac{e^{f(x)^T f(\lambda x^+ + (1-\lambda)x_j^-)}}{e^{f(x)^T f(\lambda x^+ + (1-\lambda)x_j^-)} + N g^1(x, \{x_{i_2}^-\}_i^N)}$ $-\frac{1-\lambda}{M-1} \sum_{j=1}^{M-1} \log \left(1 - \frac{e^{f(x)^T f(\lambda x^+ + (1-\lambda)x_j^-)}}{e^{f(x)^T f(\lambda x^+ + (1-\lambda)x_j^-)} + N g^1(x, \{x_{i_2}^-\}_i^N)} \right) \Big]$
$g_0(x, \{x_i^-\}_i^N)$	$\frac{1}{N} \sum_{i=1}^N e^{f(x)^T f(x_i^-)}$
$g_1(x, \{u_i\}_i^n, \{v_j\}_j^m)$	$\max \left\{ \frac{1}{1-\tau^+} \left(\frac{1}{n} \sum_{i=1}^n e^{f(x)^T f(u_i)} - \tau^+ + \frac{1}{m} \sum_{j=1}^m e^{f(x)^T f(v_j)} \right), e^{-1/t} \right\}$
$g_2(x, \{u_i\}_i^n, \{v_j\}_j^m)$	$\max \left\{ \frac{1}{1-\tau^+} \left(\frac{\sum_{i=1}^n e^{(\beta+1)f(x)^T f(u_i)}}{\sum_{i=1}^n e^{\beta f(x)^T f(u_i)}} - \tau^+ + \frac{1}{m} \sum_{j=1}^m e^{f(x)^T f(v_j)} \right), e^{-1/t} \right\}$
$\hat{w}(x)$	$-\log \frac{e^{f(x)^T f(x^+)}}{e^{f(x)^T f(x^+)} + N g(x, \cdot)}$

Notably, as the above NCA inspired contrastive losses are designed from orthogonal perspectives, they are complementary to each other. We use $\mathcal{L}_{\text{NaCl}}$ to denote these variant losses.

4 An integrated framework for contrastive learning

Building on top of our proposed NCA inspired loss (NaCl) in Section 3, we propose a useful framework that generalizes and integrates many of the existing work in contrastive learning. Our integrated contrastive learning framework has two versions, one is **IntCl** and the other is **IntNaCl**, where both of them consist of two components – a standard loss and a robustness-promoting loss. For **IntCl**, the standard loss can be existing contrastive learning loss [4, 5, 13], whereas for **IntNaCl** we use our proposed NaCl loss as the standard loss. We will show that this new framework not only generalizes existing methods but also achieves good accuracy and robustness simultaneously. Note that as shown in Figure 1(a) and 1(b), most of the existing works have primarily focused on improving the clean downstream accuracy only, which often has an undesired robustness accuracy.

4.1 Integrated contrastive loss

To design a generic loss that accounts for both clean and adversarial accuracy, together with a robustness-promoting term, we utilize the NaCl developed in Section 3 to construct a contrastive learning framework, called **Integrated Neighborhood analysis Contrastive loss (IntNaCl)**. A general form of $\mathcal{L}_{\text{IntNaCl}}$ is given by

$$\mathcal{L}_{\text{IntNaCl}}(\mathcal{L}_{\text{NaCl}}(g^1, M, \lambda), \alpha, \mathcal{L}_{\text{Robust}}(g^2, w)) := \mathcal{L}_{\text{NaCl}}(g^1, M, \lambda) + \alpha \mathcal{L}_{\text{Robust}}(g^2, w), \quad (10)$$

where $\mathcal{L}_{\text{NaCl}}(g^1, M, \lambda)$ can be chose from $\{\mathcal{L}_{\text{VAR}}(g^1, M), \mathcal{L}_{\text{BIAS}}(g^1, M), \mathcal{L}_{\text{MIXUP}}(g^1, M, \lambda)\}$ and

$$\mathcal{L}_{\text{Robust}}(g^2, w) := \mathbb{E} \left[-\log \frac{e^{f(x)^T f(x^{\text{adv}})}}{e^{f(x)^T f(x^{\text{adv}})} + N g^2(x, \cdot)} w(x) \right].$$

The variable g^1 and g^2 allow us to pick the estimators from $\{g_0, g_1, g_2\}$ and $w(x)$ facilitates goal-specific weighting scheme. Furthermore, we remark that as \mathcal{L}_{VAR} , $\mathcal{L}_{\text{BIAS}}$, and $\mathcal{L}_{\text{MIXUP}}$ all reduce to one same form when $M = 1$, we denote the $\mathcal{L}_{\text{IntNaCl}}$ under these cases by **Integrated Contrastive loss (IntCl)**:

$$\mathcal{L}_{\text{IntCl}}(\alpha, g^1, g^2, w) := \mathbb{E} \left[-\log \frac{e^{f(x)^T f(x^+)}}{e^{f(x)^T f(x^+)} + N g^1(x, \cdot)} - \alpha \log \frac{e^{f(x)^T f(x^{\text{adv}})}}{e^{f(x)^T f(x^{\text{adv}})} + N g^2(x, \cdot)} w(x) \right], \quad (11)$$

where we show many of the existing works are a special case:

$$\begin{cases} \alpha = 0, g^1 = g_0, & \mathcal{L}_{\text{SimCLR}} [4] \text{ (i.e. Equation (3));} \\ \alpha = 0, g^1 = g_1, & \mathcal{L}_{\text{Debiased}} [5] \text{ (i.e. Equation (4));} \\ \alpha = 0, g^1 = g_2, & \mathcal{L}_{\text{Debiased+HardNeg}} [13] \text{ (i.e. Equation (5));} \\ \alpha = 1, g^1 = g_0, g^2 = g_0, w(x) \equiv 1, & \mathcal{L}_{\text{Adv}} [14] \text{ (i.e. Equation (6)).} \end{cases}$$

We summarize these relationships, together with a summary of definitions in Table 1 and Table 2.

4.2 Adversarial weighting

Weighting sample loss based on their margins has been proven to be effective in the adversarial training under supervised settings [38]. Specifically, it is argued that training points that are closer to the decision boundaries should be given more weight in the supervised loss. While the margin of a sample in supervised settings is well-defined, it is underdefined in unsupervised settings. To tackle this, we borrow the intelligence from [14] and mimic how the authors transfer the definition of adversarial examples in supervised learning to unsupervised learning. Specially, we see that as an adversarial example in supervised learning is defined by a perturbed sample that has a zero margin to the decision boundary, authors of [14] define adversarial example in unsupervised learning to be an augmented sample that maximizes the contrastive loss. With this, we also give our weighting function as the value of the contrastive loss $\hat{w}(x) := -\log \frac{e^{f(x)^T f(x^+)}}{e^{f(x)^T f(x^+)} + N g(x, \cdot)}$, where the estimator g can be g_0, g_1, g_2 . Using this, we see that samples that are originally hard to be distinguished from other samples (i.e. small probability) are now assigned with bigger weights.

5 Experimental results

5.1 Experimental Set-up

Implementation details. All the proposed methods are implemented based on open source repositories provided in the literature [4, 14, 13]. Five benchmarking contrastive losses are considered as baselines that include: $\mathcal{L}_{\text{SimCLR}}$ [4], $\mathcal{L}_{\text{Debiased}}$ [5], $\mathcal{L}_{\text{Debiased+HardNeg}}$ [13], \mathcal{L}_{Adv} [14] (i.e. Equation (3), Equation (4), Equation (5), Equation (6)). We train representations on resnet18 and include MLP projection heads [4]. A batch size of 256 is used across all the experiments. Unless otherwise specified, the representation network is trained for 100 epochs. We run five independent trials for each of the experiments and report the mean and standard deviation in the entries. Throughout our experiments, no adversarial fine-tuning is performed. We implement the proposed framework using PyTorch to enable the use of an NVIDIA GeForce RTX 2080 Super GPU, two NVIDIA Tesla P100 GPUs, and four NVIDIA Tesla V100 GPUs.

Evaluation protocol. In this section, we will evaluate three major properties of representation learning methods: standard discriminative power, naive transferability, and adversarial robustness. To evaluate the standard discriminative power, we train representation networks on CIFAR100 [39], freeze the network, and only fine-tune a fully-connected layer that maps representations to outputs

Table 3: The effectiveness evaluation of NaCl on i) *Left*: SimCLR [5] (i.e. $\alpha = 0, g^1 = g_0$) and ii) *Right*: Debiased+HardNeg [13] (i.e. $\alpha = 0, g^1 = g_2$). The best performance within each loss type is in boldface. We color the overall best performance in blue.

M	$\mathcal{L}_{\text{NaCl}}(g^1, M, \lambda) = \mathcal{L}_{\text{VAR}}(g_0, M)$				$\mathcal{L}_{\text{NaCl}}(g^1, M, \lambda) = \mathcal{L}_{\text{VAR}}(g_2, M)$			
	CIFAR100 Acc.	FGSM Acc.	CIFAR10 Acc.	FGSM Acc.	CIFAR100 Acc.	FGSM Acc.	CIFAR10 Acc.	FGSM Acc.
1	53.69±0.25	25.17±0.55	76.34±0.28	43.50±0.41	56.83±0.20	31.03±0.41	77.24±0.29	48.38±0.70
2	56.04±0.17	27.19±0.79	77.32±0.14	44.61±0.33	58.17±0.39	31.92±0.45	77.43±0.18	48.05±0.38
3	57.11±0.21	27.39±0.36	78.02±0.27	44.23±0.39	59.08±0.29	32.63±0.74	77.87±0.29	47.58±0.57
4	57.27±0.14	27.63±0.78	77.91±0.29	42.97±0.61	59.29±0.16	32.48±0.62	77.92±0.17	47.08±0.53
5	57.91±0.12	28.37±0.56	78.09±0.29	44.51±0.44	59.67±0.38	33.10±0.71	78.04±0.09	46.90±0.91
M	$\mathcal{L}_{\text{NaCl}}(g^1, M, \lambda) = \mathcal{L}_{\text{BIAS}}(g_0, M)$				$\mathcal{L}_{\text{NaCl}}(g^1, M, \lambda) = \mathcal{L}_{\text{BIAS}}(g_2, M)$			
	CIFAR100 Acc.	FGSM Acc.	CIFAR10 Acc.	FGSM Acc.	CIFAR100 Acc.	FGSM Acc.	CIFAR10 Acc.	FGSM Acc.
1	53.69±0.25	25.17±0.55	76.34±0.28	43.50±0.41	56.83±0.20	31.03±0.41	77.24±0.29	48.38±0.70
2	55.72±0.15	27.04±0.45	77.40±0.14	44.58±0.41	57.87±0.15	32.50±0.48	77.43±0.11	48.14±0.31
3	56.67±0.12	28.41±0.24	77.53±0.24	45.21±0.89	58.42±0.23	33.19±0.60	77.41±0.17	48.09±0.93
4	57.09±0.26	28.20±0.81	77.75±0.22	45.13±0.44	58.86±0.18	32.65±1.07	77.46±0.29	48.43±0.94
5	57.32±0.17	28.33±0.59	77.93±0.40	44.46±0.53	58.81±0.21	32.86±0.47	77.58±0.23	48.30±0.39
M	$\mathcal{L}_{\text{NaCl}}(g^1, M, \lambda) = \mathcal{L}_{\text{MIXUP}}(g_0, M, 0.9)$				$\mathcal{L}_{\text{NaCl}}(g^1, M, \lambda) = \mathcal{L}_{\text{MIXUP}}(g_2, M, 0.5)$			
	CIFAR100 Acc.	FGSM Acc.	CIFAR10 Acc.	FGSM Acc.	CIFAR100 Acc.	FGSM Acc.	CIFAR10 Acc.	FGSM Acc.
1	53.69±0.25	25.17±0.55	76.34±0.28	43.50±0.41	56.83±0.20	31.03±0.41	77.24±0.29	48.38±0.70
2	56.20±0.33	30.95±0.36	76.96±0.15	48.85±0.75	60.69±2.43	32.22±0.35	79.36±0.65	48.86±0.34
3	56.41±0.13	30.98±0.90	77.10±0.21	48.76±0.63	59.81±0.25	32.04±0.67	79.41±0.17	48.91±0.81
4	56.00±0.42	29.90±0.63	77.11±0.40	48.16±0.40	59.75±0.33	32.03±0.34	79.42±0.18	49.05±0.71
5	56.63±0.31	30.58±0.52	77.04±0.19	47.96±0.46	59.85±0.30	32.06±0.72	79.45±0.20	48.32±0.70

Table 4: Performance comparisons of $\mathcal{L}_{\text{IntNaCl}} (M \neq 1)$ and $\mathcal{L}_{\text{IntCL}} (M = 1)$ when $\alpha = 1, g^1 = g^2 = g_2$. The best performance within each loss type is in boldface. We color the overall best performance in blue.

M	$\alpha \neq 0, \mathcal{L}_{\text{NaCl}}(g^1, M, \lambda) = \mathcal{L}_{\text{VAR}}(g_2, M)$				$\alpha \neq 0, \mathcal{L}_{\text{NaCl}}(g^1, M, \lambda) = \mathcal{L}_{\text{BIAS}}(g_2, M)$			
	CIFAR100 Acc.	FGSM Acc.	CIFAR10 Acc.	FGSM Acc.	CIFAR100 Acc.	FGSM Acc.	CIFAR10 Acc.	FGSM Acc.
1	56.22±0.15	40.05±0.67	76.39±0.10	59.33±0.94	56.22±0.15	40.05±0.67	76.39±0.10	59.33±0.94
2	57.51±0.12	41.01±0.36	76.88±0.49	58.77±0.67	56.71±0.11	39.80±0.57	76.55±0.27	58.44±0.31
3	58.08±0.18	41.02±0.83	76.95±0.19	58.28±0.50	57.13±0.26	40.53±0.29	76.67±0.22	58.47±0.31
4	58.31±0.23	41.49±0.51	77.30±0.30	58.61±0.80	57.06±0.19	40.85±0.31	76.34±0.22	58.91±0.62
5	58.64±0.24	40.50±0.23	77.42±0.17	58.11±0.72	57.46±0.04	41.00±0.86	76.60±0.37	57.98±0.47
M	$\alpha \neq 0, \mathcal{L}_{\text{NaCl}}(g^1, M, \lambda) = \mathcal{L}_{\text{MIXUP}}(g_2, M, 0.5)$				$\alpha \neq 0, \mathcal{L}_{\text{NaCl}}(g^1, M, \lambda) = \mathcal{L}_{\text{MIXUP}}(g_2, M, 0.6)$			
	CIFAR100 Acc.	FGSM Acc.	CIFAR10 Acc.	FGSM Acc.	CIFAR100 Acc.	FGSM Acc.	CIFAR10 Acc.	FGSM Acc.
1	56.22±0.15	40.05±0.67	76.39±0.10	59.33±0.94	56.22±0.15	40.05±0.67	76.39±0.10	59.33±0.94
2	58.97±0.19	40.25±0.52	78.61±0.20	58.41±0.59	58.55±0.34	40.85±0.62	78.34±0.22	59.56±0.88
3	59.26±0.18	40.96±0.58	78.83±0.22	59.20±1.25	59.05±0.21	40.83±0.44	78.41±0.12	59.14±0.78
4	59.32±0.21	40.82±0.54	78.83±0.27	59.03±0.52	59.06±0.25	40.80±0.89	78.61±0.22	58.41±1.00
5	59.43±0.23	41.01±0.34	78.80±0.21	59.51±0.93	59.10±0.23	40.68±0.50	78.63±0.21	58.92±0.76
M	$\alpha \neq 0, \mathcal{L}_{\text{NaCl}}(g^1, M, \lambda) = \mathcal{L}_{\text{MIXUP}}(g_2, M, 0.8)$				$\alpha \neq 0, \mathcal{L}_{\text{NaCl}}(g^1, M, \lambda) = \mathcal{L}_{\text{MIXUP}}(g_2, M, 0.9)$			
	CIFAR100 Acc.	FGSM Acc.	CIFAR10 Acc.	FGSM Acc.	CIFAR100 Acc.	FGSM Acc.	CIFAR10 Acc.	FGSM Acc.
1	56.22±0.15	40.05±0.67	76.39±0.10	59.33±0.94	56.22±0.15	40.05±0.67	76.39±0.10	59.33±0.94
2	57.07±0.24	41.29±0.57	77.27±0.28	60.16±0.51	56.54±0.33	40.85±0.13	76.81±0.22	60.40±0.46
3	57.62±0.22	40.93±0.49	77.54±0.27	59.47±0.52	56.69±0.11	41.23±0.66	76.98±0.22	60.13±0.56
4	57.61±0.25	41.36±0.41	77.50±0.34	60.28±0.68	56.43±0.26	41.56±0.56	76.97±0.20	61.21±0.49
5	57.56±0.18	40.71±0.34	77.58±0.42	59.99±0.30	56.86±0.11	41.09±0.31	76.91±0.21	60.09±0.39

on CIFAR100. To evaluate the transferability, we use the same representation networks as above, and only fine-tune a fully-connected layer that maps representations to outputs on CIFAR10. All the adversarial robustness evaluations are completed using the implementation provided by [40]. We supplement more FGSM and PGD attack results in the appendix.

5.2 The effectiveness of NaCl

In this section, we investigate in general the effectiveness of NaCl in improving baseline methods. For an easier assess, we let $\alpha = 0$ in Eq. (10), by doing which we eliminate the influence of the adversarial robustness module and can focus on the NaCl module. Concretely, we apply NaCl on SimCLR [4] and Debiased+HardNeg [13], and give their results in Table 3. Due to page limits, we only select one λ when $\mathcal{L}_{\text{NaCl}} = \mathcal{L}_{\text{MIXUP}}$ and report its results together with the results of $\mathcal{L}_{\text{NaCl}} = \mathcal{L}_{\text{VAR}}$ and $\mathcal{L}_{\text{NaCl}} = \mathcal{L}_{\text{BIAS}}$. Full tables can be found in the appendix. From Table 3, one can then see that \mathcal{L}_{VAR} is generally the most successful in boosting the standard accuracy when applied to SimCLR (CIFAR100: 57.91% vs. 57.32% / 56.63%, CIFAR10: 78.09 vs. 77.93% / 77.11%), whereas $\mathcal{L}_{\text{MIXUP}}$ demonstrates a better ability when applied to Debiased+HardNeg (CIFAR100: 60.69% vs. 59.67% / 58.86%, CIFAR10: 79.45% vs. 78.04% / 77.58%). Notably, by referring to the full table in the appendix, one can see that $\mathcal{L}_{\text{MIXUP}}$ with $\lambda = 0.9$ raises the CIFAR100 adversarial accuracy to 34.29% when applied to Debiased+HardNeg. That said, although \mathcal{L}_{VAR} and $\mathcal{L}_{\text{BIAS}}$ are both useful in enhancing the adversarial performance, $\mathcal{L}_{\text{MIXUP}}$ improves the baseline by the largest margin.

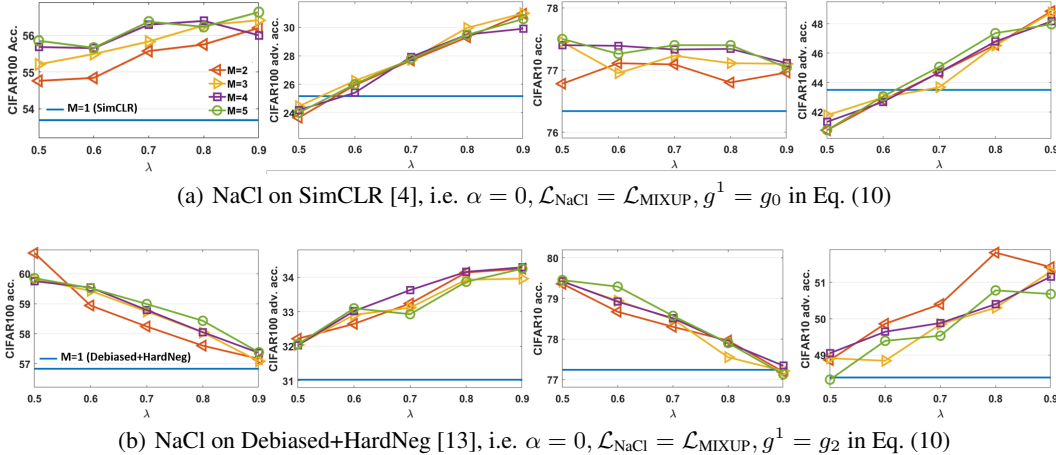


Figure 3: The standard and adversarial accuracy (%) on CIFAR100 and CIFAR10 as functions of λ in Eq. (10) when $\alpha = 0$, $\mathcal{L}_{\text{NaCl}} = \mathcal{L}_{\text{MIXUP}}$.

As training the representation with more epochs can also expose the data to more augmentations, we carry out an additional experiment to compare the efficiency and ultimate accuracy of $\mathcal{L}_{\text{NaCl}}$, $\mathcal{L}_{\text{SimCLR}}$, and $\mathcal{L}_{\text{Debiased+HardNeg}}$. In Figure S5, we give the standard accuracy of NaCl on SimCLR and NaCl on Debiased+HardNeg at different epochs. Same as before, we only select one λ when $\mathcal{L}_{\text{NaCl}} = \mathcal{L}_{\text{MIXUP}}$ and report its results together with those of $\mathcal{L}_{\text{NaCl}} = \mathcal{L}_{\text{VAR}}$ and $\mathcal{L}_{\text{NaCl}} = \mathcal{L}_{\text{BIAS}}$. In Figure S2, we plot the best standard accuracy achieved as a function of training epochs. Specially, [41] has reported a $\mathcal{L}_{\text{SimCLR}}$ CIFAR100 accuracy of 54.74% after 200 epochs, compared to $\mathcal{L}_{\text{VAR}}(g_0, 2)$'s 56.04% after 100 epochs. In our reproduction of the $\mathcal{L}_{\text{SimCLR}}$ 200-epoch result², we have witnessed an accuracy of 57.45% however at the cost of 1.34X training time (cf. 200 epochs with $\mathcal{L}_{\text{SimCLR}}$ takes 211 mins vs. 100 epochs with $\mathcal{L}_{\text{VAR}}(g_0, 2)$ takes 158 mins). Overall, we see that NaCl methods demonstrate better efficiency when applying on SimCLR and better ultimate accuracy when applying on Debiased+HardNeg.

To further investigate the effect of λ on different accuracy metrics, we include in Figure 3 the standard and adversarial accuracy on CIFAR100 and CIFAR10 as functions of λ . Intriguingly, we see that the accuracy curves mainly show trends of increasing in Figure 3(a). Comparatively, the standard accuracy on CIFAR100 and CIFAR10 shows trends of decreasing in Figure 3(b). One possible explanation is by the original baselines' room for improvement. Since Debiased+HardNeg is a much stronger baseline than SimCLR, it is closer to the robustness-accuracy trade-off. However, we note that the overall performance of NaCl on Debiased+HardNeg is still better than NaCl on SimCLR regardless of the robustness-accuracy trade-off.

5.3 $\mathcal{L}_{\text{IntNaCl}}$ and $\mathcal{L}_{\text{IntCL}}$ learn representations with robustness property

In Figure 1, we plot the adversarial accuracy defined under FGSM attacks [26] along the y-axis. Ideally, one will want a representation network that pushes the performance to the upper-right corner in the 2D accuracy grid (standard-adversarial accuracy plot). Now, we see that SimCLR, Debiased, HardNeg, and Debiased+HardNeg all score relatively poorly, obtaining an adversarial accuracy of around or below 30% on CIFAR100 and 50% on CIFAR10. One exception, Adv, performs adequately and reaches an accuracy of more than 35% on CIFAR100 and 55% on CIFAR10, while sacrificing the standard accuracy. We highlight the results of $\mathcal{L}_{\text{IntNaCl}}$ and $\mathcal{L}_{\text{IntCL}}$ in circles, through which we see that while $\mathcal{L}_{\text{IntCL}}$ can already train representations that are decently robust without sacrificing the standard accuracy on CIFAR100, the standard accuracy on CIFAR10 is inferior to some baselines (HardNeg and Debiased+HardNeg). Comparatively, $\mathcal{L}_{\text{IntNaCl}}$ wins over the baselines by a large margin on both datasets, proving the ability of learning representation networks that also transfer robustness property.

²We let the dataloader shuffle the whole dataset to form new batches after every epoch, so by doubling the training epoch, one will effectively expose the network to more diverse negative pairs.

5.4 Comparing $\mathcal{L}_{\text{IntNaCl}}$ and $\mathcal{L}_{\text{IntCL}}$

In Figure 1, we only show the result of $\mathcal{L}_{\text{IntNaCl}}$ when $\alpha = 1$, $\mathcal{L}_{\text{NaCl}}(g^1, M, \lambda) = \mathcal{L}_{\text{MIXUP}}(g_2, 5, 0.5)$ and $\mathcal{L}_{\text{Robust}}(g^2, w) = \mathcal{L}_{\text{Robust}}(g_2, w(x))$, where $w(x)$ is as defined in Section 4.2. Correspondingly, the representative of $\mathcal{L}_{\text{IntCL}}$ is given by inheriting the above parameter choices but setting $M = 1$. In this section, while we still conduct experiments with the same $\alpha = 1$, $\mathcal{L}_{\text{Robust}}(g_2, w(x))$, and $g^1 = g_2$, we vary $\mathcal{L}_{\text{NaCl}}(g_2, M, \lambda)$ from $\{\mathcal{L}_{\text{VAR}}(g_2, M), \mathcal{L}_{\text{BIAS}}(g_2, M), \mathcal{L}_{\text{MIXUP}}(g_2, M, \lambda)\}$ and report their performance in Table 4. Specifically, the representation network learned via $\mathcal{L}_{\text{IntCL}}$ leads to a standard accuracy of 56.22% and an adversarial accuracy of 40.05% under FGSM attacks with magnitude $\epsilon = 0.002$ on CIFAR100. When using the same representation network on CIFAR10, one obtains a transfer standard accuracy of 76.39% and a transfer adversarial accuracy of 59.33%. Although $\mathcal{L}_{\text{IntNaCl}}$ generally improves upon $\mathcal{L}_{\text{IntCL}}$ in all metrics as shown by the results when $\mathcal{L}_{\text{NaCl}} = \mathcal{L}_{\text{MIXUP}}$, we see that when we set $\mathcal{L}_{\text{NaCl}}$ to be \mathcal{L}_{VAR} or $\mathcal{L}_{\text{BIAS}}$, the transfer adversarial accuracy might decrease.

6 Conclusion

In this paper, we discover the relationship between contrastive loss and Neighborhood Component Analysis (NCA), which motivates us to generalize the existing contrastive loss to a set of Neighborhood analysis Contrastive losses (NaCl). We further propose a generic contrastive learning framework based on NaCl, which learns representations that score high in both standard accuracy and adversarial accuracy in downstream tasks. Future work includes addressing the current limitation of assuming $k = 1$ for k-nearest neighbor in NCA to $k > 1$ [42], by doing which we expect to extend the current framework to an even more general form.

References

- [1] A. v. d. Oord, Y. Li, and O. Vinyals, “Representation learning with contrastive predictive coding,” *arXiv preprint arXiv:1807.03748*, 2018.
- [2] Z. Wu, Y. Xiong, S. X. Yu, and D. Lin, “Unsupervised feature learning via non-parametric instance discrimination,” in *CVPR*, pp. 3733–3742, 2018.
- [3] K. He, H. Fan, Y. Wu, S. Xie, and R. Girshick, “Momentum contrast for unsupervised visual representation learning,” in *CVPR*, June 2020.
- [4] T. Chen, S. Kornblith, M. Norouzi, and G. Hinton, “A simple framework for contrastive learning of visual representations,” in *ICML*, vol. 119 of *Proceedings of Machine Learning Research*, (Virtual), pp. 1597–1607, PMLR, 13–18 Jul 2020.
- [5] C.-Y. Chuang, J. Robinson, L. Yen-Chen, A. Torralba, and S. Jegelka, “Debiased contrastive learning,” *arXiv preprint arXiv:2007.00224*, 2020.
- [6] J.-B. Grill, F. Strub, F. Altché, C. Tallec, P. Richemond, E. Buchatskaya, C. Doersch, B. Avila Pires, Z. Guo, M. Gheshlaghi Azar, B. Piot, k. kavukcuoglu, R. Munos, and M. Valko, “Bootstrap your own latent - a new approach to self-supervised learning,” in *NeurIPS*, vol. 33, pp. 21271–21284, 2020.
- [7] A. Dosovitskiy, P. Fischer, J. T. Springenberg, M. Riedmiller, and T. Brox, “Discriminative unsupervised feature learning with exemplar convolutional neural networks,” *IEEE transactions on pattern analysis and machine intelligence*, vol. 38, no. 9, pp. 1734–1747, 2015.
- [8] P. Bojanowski and A. Joulin, “Unsupervised learning by predicting noise,” in *ICML*, pp. 517–526, PMLR, 2017.
- [9] X. Chen, H. Fan, R. B. Girshick, and K. He, “Improved baselines with momentum contrastive learning,” *CoRR*, vol. abs/2003.04297, 2020.
- [10] X. Wang and A. Gupta, “Unsupervised learning of visual representations using videos,” in *Proceedings of the IEEE international conference on computer vision*, pp. 2794–2802, 2015.
- [11] M. Ye, X. Zhang, P. C. Yuen, and S.-F. Chang, “Unsupervised embedding learning via invariant and spreading instance feature,” in *Proceedings of the IEEE/CVF Conference on Computer Vision and Pattern Recognition*, pp. 6210–6219, 2019.
- [12] J. Goldberger, G. E. Hinton, S. Roweis, and R. R. Salakhutdinov, “Neighbourhood components analysis,” *NeurIPS*, vol. 17, pp. 513–520, 2004.

- [13] J. D. Robinson, C.-Y. Chuang, S. Sra, and S. Jegelka, “Contrastive learning with hard negative samples,” in *ICLR*, 2021.
- [14] C.-H. Ho and N. Vasconcelos, “Contrastive learning with adversarial examples,” *arXiv preprint arXiv:2010.12050*, 2020.
- [15] M. Gutmann and A. Hyvärinen, “Noise-contrastive estimation: A new estimation principle for unnormalized statistical models,” in *Proceedings of the Thirteenth International Conference on Artificial Intelligence and Statistics*, pp. 297–304, JMLR Workshop and Conference Proceedings, 2010.
- [16] A. Mnih and Y. W. Teh, “A fast and simple algorithm for training neural probabilistic language models,” in *ICML*, 2012.
- [17] R. Jozefowicz, O. Vinyals, M. Schuster, N. Shazeer, and Y. Wu, “Exploring the limits of language modeling,” *arXiv preprint arXiv:1602.02410*, 2016.
- [18] M. Caron, I. Misra, J. Mairal, P. Goyal, P. Bojanowski, and A. Joulin, “Unsupervised learning of visual features by contrasting cluster assignments,” in *NeurIPS*, vol. 33, pp. 9912–9924, 2020.
- [19] N. Saunshi, O. Plevrakis, S. Arora, M. Khodak, and H. Khandeparkar, “A theoretical analysis of contrastive unsupervised representation learning,” in *ICML*, pp. 5628–5637, 2019.
- [20] M. Kim, J. Tack, and S. J. Hwang, “Adversarial self-supervised contrastive learning,” *arXiv preprint arXiv:2006.07589*, 2020.
- [21] L. Fan, S. Liu, P.-Y. Chen, G. Zhang, and C. Gan, “When does contrastive learning preserve adversarial robustness from pretraining to finetuning?,” 2021.
- [22] H. Kannan, A. Kurakin, and I. J. Goodfellow, “Adversarial logit pairing,” *CoRR*, vol. abs/1803.06373, 2018.
- [23] P. Khosla, P. Teterwak, C. Wang, A. Sarna, Y. Tian, P. Isola, A. Maschinot, C. Liu, and D. Krishnan, “Supervised contrastive learning,” *arXiv preprint arXiv:2004.11362*, 2020.
- [24] Y. Tian, C. Sun, B. Poole, D. Krishnan, C. Schmid, and P. Isola, “What makes for good views for contrastive learning?,” in *NeurIPS*, vol. 33, pp. 6827–6839, 2020.
- [25] D. Dwibedi, Y. Aytar, J. Tompson, P. Sermanet, and A. Zisserman, “With a little help from my friends: Nearest-neighbor contrastive learning of visual representations,” 2021.
- [26] I. Goodfellow, J. Shlens, and C. Szegedy, “Explaining and harnessing adversarial examples,” in *ICLR*, 2015.
- [27] C. Szegedy, W. Zaremba, I. Sutskever, J. Bruna, D. Erhan, I. Goodfellow, and R. Fergus, “Intriguing properties of neural networks,” in *ICLR*, 2014.
- [28] A. Nguyen, J. Yosinski, and J. Clune, “Deep neural networks are easily fooled: High confidence predictions for unrecognizable images,” in *CVPR*, 2015.
- [29] S.-M. Moosavi-Dezfooli, A. Fawzi, and P. Frossard, “Deepfool: a simple and accurate method to fool deep neural networks,” in *CVPR*, pp. 2574–2582, 2016.
- [30] A. Madry, A. Makelov, L. Schmidt, D. Tsipras, and A. Vladu, “Towards deep learning models resistant to adversarial attacks,” in *ICLR*, 2018.
- [31] A. Kurakin, I. J. Goodfellow, and S. Bengio, “Adversarial machine learning at scale,” in *ICLR*, 2016.
- [32] K. Sohn, “Improved deep metric learning with multi-class n-pair loss objective,” in *NeurIPS*, vol. 29, 2016.
- [33] Y. Tian, D. Krishnan, and P. Isola, “Contrastive multiview coding,” in *Computer Vision—ECCV 2020: 16th European Conference, Glasgow, UK, August 23–28, 2020, Proceedings, Part XI 16*, pp. 776–794, Springer, 2020.
- [34] K. Hassani and A. H. Khasahmadi, “Contrastive multi-view representation learning on graphs,” in *International Conference on Machine Learning*, pp. 4116–4126, PMLR, 2020.
- [35] H. Zhang, M. Cisse, Y. N. Dauphin, and D. Lopez-Paz, “mixup: Beyond empirical risk minimization,” in *ICLR*, 2018.
- [36] K. Lee, Y. Zhu, K. Sohn, C.-L. Li, J. Shin, and H. Lee, “\$i\$-mix: A domain-agnostic strategy for contrastive representation learning,” in *ICLR*, 2021.

- [37] V. Verma, T. Luong, K. Kawaguchi, H. Pham, and Q. Le, “Towards domain-agnostic contrastive learning,” in *International Conference on Machine Learning*, pp. 10530–10541, PMLR, 2021.
- [38] H. Zeng, C. Zhu, T. Goldstein, and F. Huang, “Are adversarial examples created equal? a learnable weighted minimax risk for robustness under non-uniform attacks,” *arXiv preprint arXiv:2010.12989*, 2020.
- [39] A. Krizhevsky, G. Hinton, *et al.*, “Learning multiple layers of features from tiny images,” 2009.
- [40] E. Wong, L. Rice, and J. Z. Kolter, “Fast is better than free: Revisiting adversarial training,” in *ICLR*, 2020.
- [41] J. Z. HaoChen, C. Wei, A. Gaidon, and T. Ma, “Provable guarantees for self-supervised deep learning with spectral contrastive loss,” *arXiv preprint arXiv:2106.04156*, 2021.
- [42] D. Tarlow, K. Swersky, L. Charlin, I. Sutskever, and R. Zemel, “Stochastic k-neighborhood selection for supervised and unsupervised learning,” in *ICML*, 2013.

A Derivation from Eq. (8) to (9)

$$\begin{aligned} & \arg \min_f \sum_{i=1}^n -\log \left(\frac{\sum_{j=1}^M e^{-\frac{1}{2}\|f(x_i)-f(x_j^+)\|^2}}{\sum_{k \neq i} e^{-\frac{1}{2}\|f(x_i)-f(x_k)\|^2}} \right) \\ &= \arg \min_f \sum_{i=1}^n -\log \left(\frac{\sum_{j=1}^M \frac{e^{f(x_i)^T f(x_j^+) - \frac{1}{2}\|f(x_i)\|^2 - \frac{1}{2}\|f(x_j^+)\|^2}}{\sum_{k \neq i} e^{f(x_i)^T f(x_k) - \frac{1}{2}\|f(x_i)\|^2 - \frac{1}{2}\|f(x_k)\|^2}} \right) \end{aligned} \quad (\text{S1})$$

$$= \arg \min_f \sum_{i=1}^n -\log \left(\frac{\sum_{j=1}^M \frac{e^{f(x_i)^T f(x_j^+) - 1}}{\sum_{k \neq i} e^{f(x_i)^T f(x_k) - 1}} \right) \quad (\text{S2})$$

$$\begin{aligned} &= \arg \min_f \sum_{i=1}^n -\log \left(\frac{\sum_{j=1}^M e^{f(x_i)^T f(x_j^+)}}{\sum_{k \neq i} e^{f(x_i)^T f(x_k)}} \right) \\ &= \arg \min_f \sum_{i=1}^n -\log \left(\frac{\sum_{j=1}^M e^{f(x_i)^T f(x_j^+)}}{\sum_{k \neq i, x_k \in \{x_j^+\}} e^{f(x_i)^T f(x_k)} + \sum_{k \neq i, x_k \notin \{x_j^+\}} e^{f(x_i)^T f(x_k)}} \right) \end{aligned} \quad (\text{S3})$$

$$= \arg \min_f \mathbb{E}_{x \sim \mathcal{D}} \left[-\log \left(\frac{\sum_{j=1}^M e^{f(x)^T f(x_j^+)}}{\sum_{j=1}^M e^{f(x)^T f(x_j^+)} + \sum_{i=1}^N e^{f(x)^T f(x_i^-)}} \right) \right] \quad (\text{S4})$$

$$= \arg \min_f \mathbb{E}_{x \sim \mathcal{D}} \left[-\log \left(\frac{\sum_{j=1}^M e^{f(x)^T f(x_j^+)}}{\sum_{j=1}^M e^{f(x)^T f(x_j^+)} + N g_0(x, \{x_i^-\}_N)} \right) \right],$$

where we go from Equation (S1) to Equation (S2) based on the fact that $\|f(x)\| = 1$, and from Equation (S3) to Equation (S4) assuming that set $\{x_k : k \neq i\} = \{x_j^+ : 1 \leq j \leq M\} \cup \{x_i^- : 1 \leq i \leq N\}$.

B Complete tables of results

We give the full table of results in Section 5 in the following. Notably, we gather the standard accuracy, adversarial accuracy, transfer accuracy, and transfer adversarial accuracy for each specification.

Table S1: The effectiveness evaluation of NaCl on SimCLR (i.e. $\alpha = 0, g^1 = g_0$). The best performance within each loss type is in boldface. We color the overall best performance in blue.

M	$\alpha = 0, \mathcal{L}_{\text{NaCl}}(g_0, M, \lambda) = \mathcal{L}_{\text{VAR}}(g_0, M)$			
	CIFAR100 Acc.	FGSM Acc.	CIFAR10 Acc.	FGSM Acc.
1	53.69±0.25	25.17±0.55	76.34±0.28	43.50±0.41
2	56.04±0.17	27.19±0.79	77.32±0.14	44.61±0.33
3	57.11±0.21	27.39±0.36	78.02±0.27	44.23±0.39
4	57.27±0.14	27.63±0.78	77.91±0.29	42.97±0.61
5	57.91±0.12	28.37±0.56	78.09±0.29	44.51±0.44
	$\alpha = 0, \mathcal{L}_{\text{NaCl}}(g_0, M, \lambda) = \mathcal{L}_{\text{BIAS}}(g_0, M)$			
1	53.69±0.25	25.17±0.55	76.34±0.28	43.50±0.41
2	55.72±0.15	27.04±0.45	77.40±0.14	44.58±0.41
3	56.67±0.12	28.41±0.24	77.53±0.24	45.21±0.89
4	57.09±0.26	28.20±0.81	77.75±0.22	45.13±0.44
5	57.32±0.17	28.33±0.59	77.93±0.40	44.46±0.53
	$\alpha = 0, \mathcal{L}_{\text{NaCl}}(g_0, M, \lambda) = \mathcal{L}_{\text{MIXUP}}(g_0, M, 0.5)$			
1	53.69±0.25	25.17±0.55	76.34±0.28	43.50±0.41
2	54.76±0.29	23.66±0.27	76.78±0.26	40.76±0.66
3	55.21±0.17	24.46±0.44	77.45±0.18	41.78±0.80
4	55.68±0.27	24.19±0.46	77.40±0.24	41.33±0.34
5	55.85±0.16	24.01±0.91	77.50±0.16	40.77±0.66
	$\alpha = 0, \mathcal{L}_{\text{NaCl}}(g_0, M, \lambda) = \mathcal{L}_{\text{MIXUP}}(g_0, M, 0.6)$			
1	53.69±0.25	25.17±0.55	76.34±0.28	43.50±0.41
2	54.84±0.35	25.94±0.81	77.11±0.15	42.81±0.83
3	55.49±0.13	26.25±0.89	76.95±0.32	42.99±0.96
4	55.65±0.24	25.41±0.53	77.39±0.37	42.69±1.20
5	55.66±0.22	26.01±0.60	77.26±0.48	43.06±0.79
	$\alpha = 0, \mathcal{L}_{\text{NaCl}}(g_0, M, \lambda) = \mathcal{L}_{\text{MIXUP}}(g_0, M, 0.7)$			
1	53.69±0.25	25.17±0.55	76.34±0.28	43.50±0.41
2	55.57±0.32	27.67±0.60	77.09±0.27	44.68±0.71
3	55.83±0.25	27.72±0.59	77.23±0.28	43.68±0.72
4	56.29±0.25	27.92±0.60	77.33±0.29	44.69±0.82
5	56.37±0.32	27.78±0.54	77.40±0.20	45.07±0.98
	$\alpha = 0, \mathcal{L}_{\text{NaCl}}(g_0, M, \lambda) = \mathcal{L}_{\text{MIXUP}}(g_0, M, 0.8)$			
1	53.69±0.25	25.17±0.55	76.34±0.28	43.50±0.41
2	55.75±0.21	29.30±0.86	76.80±0.20	46.56±1.02
3	56.27±0.26	29.96±0.29	77.11±0.37	46.52±0.50
4	56.39±0.26	29.49±0.65	77.34±0.31	46.79±0.93
5	56.23±0.13	29.47±0.95	77.40±0.14	47.36±0.69
	$\alpha = 0, \mathcal{L}_{\text{NaCl}}(g_0, M, \lambda) = \mathcal{L}_{\text{MIXUP}}(g_0, M, 0.9)$			
1	53.69±0.25	25.17±0.55	76.34±0.28	43.50±0.41
2	56.20±0.33	30.95±0.36	76.96±0.15	48.85±0.75
3	56.41±0.13	30.98±0.90	77.10±0.21	48.76±0.63
4	56.00±0.42	29.90±0.63	77.11±0.40	48.16±0.40
5	56.63±0.31	30.58±0.52	77.04±0.19	47.96±0.46

Table S2: The effectiveness evaluation of NaCl on Debised+HardNeg (i.e. $\alpha = 0, g^1 = g_2$). The best performance within each loss type is in boldface. We color the overall best performance in blue.

M	$\alpha = 0, \mathcal{L}_{\text{NaCl}}(g_2, M, \lambda) = \mathcal{L}_{\text{VAR}}(g_2, M)$			
	CIFAR100 Acc.	FGSM Acc.	CIFAR10 Acc.	FGSM Acc.
1	56.83±0.20	31.03±0.41	77.24±0.29	48.38±0.70
2	58.17±0.39	31.92±0.45	77.43±0.18	48.05±0.38
3	59.08±0.29	32.63±0.74	77.87±0.29	47.58±0.57
4	59.29±0.16	32.48±0.62	77.92±0.17	47.08±0.53
5	59.67±0.38	33.10±0.71	78.04±0.09	46.90±0.91
	$\alpha = 0, \mathcal{L}_{\text{NaCl}}(g_2, M, \lambda) = \mathcal{L}_{\text{BIAS}}(g_2, M)$			
1	56.83±0.20	31.03±0.41	77.24±0.29	48.38±0.70
2	57.87±0.15	32.50±0.48	77.43±0.11	48.14±0.31
3	58.42±0.23	33.19±0.60	77.41±0.17	48.09±0.93
4	58.86±0.18	32.65±1.07	77.46±0.29	48.43±0.94
5	58.81±0.21	32.86±0.47	77.58±0.23	48.30±0.39
	$\alpha = 0, \mathcal{L}_{\text{NaCl}}(g_2, M, \lambda) = \mathcal{L}_{\text{MIXUP}}(g_2, M, 0.5)$			
1	56.83±0.20	31.03±0.41	77.24±0.29	48.38±0.70
2	60.69±0.43	32.22±0.35	79.36±0.65	48.86±0.34
3	59.81±0.25	32.04±0.67	79.41±0.17	48.91±0.81
4	59.75±0.33	32.03±0.34	79.42±0.18	49.05±0.71
5	59.85±0.30	32.06±0.72	79.45±0.20	48.32±0.70
	$\alpha = 0, \mathcal{L}_{\text{NaCl}}(g_2, M, \lambda) = \mathcal{L}_{\text{MIXUP}}(g_2, M, 0.6)$			
1	56.83±0.20	31.03±0.41	77.24±0.29	48.38±0.70
2	58.94±0.29	32.65±0.36	78.67±0.15	49.86±0.59
3	59.43±0.35	32.91±0.40	78.94±0.19	48.84±1.09
4	59.54±0.28	33.02±0.62	78.92±0.29	49.64±0.74
5	59.52±0.28	33.10±0.50	79.29±0.21	49.39±1.02
	$\alpha = 0, \mathcal{L}_{\text{NaCl}}(g_2, M, \lambda) = \mathcal{L}_{\text{MIXUP}}(g_2, M, 0.7)$			
1	56.83±0.20	31.03±0.41	77.24±0.29	48.38±0.70
2	58.24±0.19	33.24±0.90	78.30±0.31	50.40±0.83
3	58.74±0.26	33.12±0.59	78.49±0.30	49.85±0.38
4	58.79±0.38	33.63±0.53	78.51±0.29	49.88±0.75
5	58.99±0.18	32.93±0.81	78.57±0.12	49.53±1.55
	$\alpha = 0, \mathcal{L}_{\text{NaCl}}(g_2, M, \lambda) = \mathcal{L}_{\text{MIXUP}}(g_2, M, 0.8)$			
1	56.83±0.20	31.03±0.41	77.24±0.29	48.38±0.70
2	57.60±0.15	34.14±0.22	77.96±0.07	51.82±0.68
3	58.04±0.28	33.93±0.45	77.55±0.18	50.30±0.81
4	58.05±0.16	34.16±0.54	77.90±0.21	50.40±0.43
5	58.43±0.27	33.87±0.62	77.90±0.17	50.78±0.95
	$\alpha = 0, \mathcal{L}_{\text{NaCl}}(g_2, M, \lambda) = \mathcal{L}_{\text{MIXUP}}(g_2, M, 0.9)$			
1	56.83±0.20	31.03±0.41	77.24±0.29	48.38±0.70
2	57.16±0.15	34.25±0.55	77.19±0.09	51.42±0.45
3	57.08±0.10	33.96±0.19	77.21±0.26	51.30±1.05
4	57.36±0.19	34.29±0.15	77.34±0.34	51.16±0.55
5	57.38±0.16	34.25±0.30	77.13±0.16	50.68±0.74

Table S3: The effectiveness evaluation of NaCl ($M \neq 1$) on IntCl ($M = 1$) when $\alpha = 1, g^1 = g^2 = g_2$. The best performance within each loss type is in boldface. We color the overall best performance in blue.

M	$\alpha \neq 0, \mathcal{L}_{\text{NaCl}}(g_2, M, \lambda) = \mathcal{L}_{\text{VAR}}(g_2, M)$			
	CIFAR100 Acc.	FGSM Acc.	CIFAR10 Acc.	FGSM Acc.
1	56.22±0.15	40.05±0.67	76.39±0.10	59.33±0.94
2	57.51±0.12	41.01±0.36	76.88±0.49	58.77±0.67
3	58.08±0.18	41.02±0.83	76.95±0.19	58.28±0.50
4	58.31±0.23	41.49±0.51	77.30±0.30	58.61±0.80
5	58.64±0.24	40.50±0.23	77.42±0.17	58.11±0.72
$\alpha \neq 0, \mathcal{L}_{\text{NaCl}}(g_2, M, \lambda) = \mathcal{L}_{\text{BIAS}}(g_2, M)$				
1	56.22±0.15	40.05±0.67	76.39±0.10	59.33±0.94
2	56.71±0.11	39.80±0.57	76.55±0.27	58.44±0.31
3	57.13±0.26	40.53±0.29	76.67±0.22	58.47±0.31
4	57.06±0.19	40.85±0.31	76.34±0.22	58.91±0.62
5	57.46±0.04	41.00±0.86	76.60±0.37	57.98±0.47
$\alpha \neq 0, \mathcal{L}_{\text{NaCl}}(g_2, M, \lambda) = \mathcal{L}_{\text{MIXUP}}(g_2, M, 0.5)$				
1	56.22±0.15	40.05±0.67	76.39±0.10	59.33±0.94
2	58.97±0.19	40.25±0.52	78.61±0.20	58.41±0.59
3	59.26±0.18	40.96±0.58	78.83±0.22	59.20±1.25
4	59.32±0.21	40.82±0.54	78.83±0.27	59.03±0.52
5	59.43±0.23	41.01±0.34	78.80±0.21	59.51±0.93
$\alpha \neq 0, \mathcal{L}_{\text{NaCl}}(g_2, M, \lambda) = \mathcal{L}_{\text{MIXUP}}(g_2, M, 0.6)$				
1	56.22±0.15	40.05±0.67	76.39±0.10	59.33±0.94
2	58.55±0.34	40.85±0.62	78.34±0.22	59.56±0.88
3	59.05±0.21	40.83±0.44	78.41±0.12	59.14±0.78
4	59.06±0.25	40.80±0.89	78.61±0.22	58.41±1.00
5	59.10±0.23	40.68±0.50	78.63±0.21	58.92±0.76
$\alpha \neq 0, \mathcal{L}_{\text{NaCl}}(g_2, M, \lambda) = \mathcal{L}_{\text{MIXUP}}(g_2, M, 0.7)$				
1	56.22±0.15	40.05±0.67	76.39±0.10	59.33±0.94
2	58.00±0.18	40.35±0.34	77.73±0.24	59.40±1.27
3	58.23±0.18	40.94±0.75	77.91±0.25	59.57±0.81
4	58.20±0.25	40.95±0.45	77.89±0.20	59.49±0.49
5	58.37±0.14	41.15±0.48	78.27±0.26	59.17±0.94
$\alpha \neq 0, \mathcal{L}_{\text{NaCl}}(g_2, M, \lambda) = \mathcal{L}_{\text{MIXUP}}(g_2, M, 0.8)$				
1	56.22±0.15	40.05±0.67	76.39±0.10	59.33±0.94
2	57.07±0.24	41.29±0.57	77.27±0.28	60.16±0.51
3	57.62±0.22	40.93±0.49	77.54±0.27	59.47±0.52
4	57.61±0.25	41.36±0.41	77.50±0.34	60.28±0.68
5	57.56±0.18	40.71±0.34	77.58±0.42	59.99±0.30
$\alpha \neq 0, \mathcal{L}_{\text{NaCl}}(g_2, M, \lambda) = \mathcal{L}_{\text{MIXUP}}(g_2, M, 0.9)$				
1	56.22±0.15	40.05±0.67	76.39±0.10	59.33±0.94
2	56.54±0.33	40.85±0.13	76.81±0.22	60.40±0.46
3	56.69±0.11	41.23±0.66	76.98±0.22	60.13±0.56
4	56.43±0.26	41.56±0.56	76.97±0.20	61.21±0.49
5	56.86±0.11	41.09±0.31	76.91±0.21	60.09±0.39

C Adversarial accuracy

For a more comprehensive study of adversarial robustness, we extend Table S2 to include PGD attack results with the same strength as FGSM attacks ($\epsilon = 0.002$). One can readily see from Table S4 that the adversarial accuracy under PGD attacks of the same magnitude is slightly lower (roughly 2-3% lower) as PGD is a stronger attack. Nevertheless, the trend is consistent – the models that exhibit better adversarial robustness w.r.t. FGSM attacks also demonstrate superior adversarial robustness w.r.t. PGD attacks.

Table S4: The complete Table S2 (Table 1 right column) with additional PGD accuracy.

M	$\alpha = 0, \mathcal{L}_{\text{NaCl}}(g_2, M, \lambda) = \mathcal{L}_{\text{VAR}}(g_2, M)$					
	CIFAR100 Acc.	FGSM Acc.	PGD Acc.	CIFAR10 Acc.	FGSM Acc.	PGD Acc.
1	56.83±0.20	31.03±0.41	28.80±0.48	77.24±0.29	48.38±0.70	46.24±0.77
2	58.17±0.39	31.92±0.45	29.77±0.43	77.43±0.18	48.05±0.38	45.63±0.50
3	59.08±0.29	32.63±0.74	30.33±0.84	77.87±0.29	47.58±0.57	45.02±0.62
4	59.29±0.16	32.48±0.62	30.12±0.73	77.92±0.17	47.08±0.53	44.52±0.54
5	59.67±0.38	33.10±0.71	30.87±0.88	78.04±0.09	46.90±0.91	44.20±1.08
	$\alpha = 0, \mathcal{L}_{\text{NaCl}}(g_2, M, \lambda) = \mathcal{L}_{\text{BIAS}}(g_2, M)$					
1	56.83±0.20	31.03±0.41	28.80±0.48	77.24±0.29	48.38±0.70	46.24±0.77
2	57.87±0.15	32.50±0.48	30.25±0.60	77.43±0.11	48.14±0.31	45.81±0.43
3	58.42±0.23	33.19±0.60	30.93±0.59	77.41±0.17	48.09±0.93	45.67±0.93
4	58.86±0.18	32.65±1.07	30.22±1.09	77.46±0.29	48.43±0.94	45.99±1.15
5	58.81±0.21	32.86±0.47	30.57±0.55	77.58±0.23	48.30±0.39	45.80±0.48
	$\alpha = 0, \mathcal{L}_{\text{NaCl}}(g_2, M, \lambda) = \mathcal{L}_{\text{MIXUP}}(g_2, M, 0.5)$					
1	56.83±0.20	31.03±0.41	28.80±0.48	77.24±0.29	48.38±0.70	46.24±0.77
2	60.69±0.43	32.22±0.35	30.11±0.43	79.36±0.65	48.86±0.34	46.67±0.40
3	59.81±0.25	32.04±0.67	29.87±0.65	79.41±0.17	48.91±0.81	46.61±0.86
4	59.75±0.33	32.03±0.34	29.85±0.36	79.42±0.18	49.05±0.71	46.70±0.80
5	59.85±0.30	32.06±0.72	29.99±0.76	79.45±0.20	48.32±0.70	45.89±0.82
	$\alpha = 0, \mathcal{L}_{\text{NaCl}}(g_2, M, \lambda) = \mathcal{L}_{\text{MIXUP}}(g_2, M, 0.6)$					
1	56.83±0.20	31.03±0.41	28.80±0.48	77.24±0.29	48.38±0.70	46.24±0.77
2	58.94±0.29	32.65±0.36	30.16±0.27	78.67±0.15	49.86±0.59	47.38±0.70
3	59.43±0.35	32.91±0.40	30.36±0.52	78.94±0.19	48.84±1.09	46.24±1.32
4	59.54±0.28	33.02±0.62	30.68±0.72	78.92±0.29	49.64±0.74	47.15±0.88
5	59.52±0.28	33.10±0.50	30.63±0.48	79.29±0.21	49.39±1.02	46.89±1.12
	$\alpha = 0, \mathcal{L}_{\text{NaCl}}(g_2, M, \lambda) = \mathcal{L}_{\text{MIXUP}}(g_2, M, 0.7)$					
1	56.83±0.20	31.03±0.41	28.80±0.48	77.24±0.29	48.38±0.70	46.24±0.77
2	58.24±0.19	33.24±0.90	30.40±1.06	78.30±0.31	50.40±0.83	47.50±0.89
3	58.74±0.26	33.12±0.59	29.94±0.62	78.49±0.30	49.85±0.38	46.69±0.32
4	58.79±0.38	33.63±0.53	30.70±0.60	78.51±0.29	49.88±0.75	47.01±0.96
5	58.99±0.18	32.93±0.81	29.89±0.99	78.57±0.12	49.53±1.55	46.41±1.91
	$\alpha = 0, \mathcal{L}_{\text{NaCl}}(g_2, M, \lambda) = \mathcal{L}_{\text{MIXUP}}(g_2, M, 0.8)$					
1	56.83±0.20	31.03±0.41	28.80±0.48	77.24±0.29	48.38±0.70	46.24±0.77
2	57.60±0.15	34.14±0.22	31.35±0.25	77.96±0.07	51.82±0.68	48.81±0.85
3	58.04±0.28	33.93±0.45	31.31±0.62	77.55±0.18	50.30±0.81	47.41±0.76
4	58.05±0.16	34.16±0.54	31.41±0.61	77.90±0.21	50.40±0.43	47.58±0.47
5	58.43±0.27	33.87±0.62	31.23±0.76	77.90±0.17	50.78±0.95	47.96±1.12
	$\alpha = 0, \mathcal{L}_{\text{NaCl}}(g_2, M, \lambda) = \mathcal{L}_{\text{MIXUP}}(g_2, M, 0.9)$					
1	56.83±0.20	31.03±0.41	28.80±0.48	77.24±0.29	48.38±0.70	46.24±0.77
2	57.16±0.15	34.25±0.55	31.83±0.57	77.19±0.09	51.42±0.45	49.09±0.53
3	57.08±0.10	33.96±0.19	31.56±0.34	77.21±0.26	51.30±1.05	48.60±1.28
4	57.36±0.19	34.29±0.15	31.93±0.32	77.34±0.34	51.16±0.55	48.64±0.61
5	57.38±0.16	34.25±0.30	31.89±0.26	77.13±0.16	50.68±0.74	48.14±0.83

In Figure S1, we show the adversarial accuracy as a function of the FGSM attack strength ϵ . Specifically, we range the attack strength from 0.002 to 0.032 and give the adversarial accuracy of our proposals (IntCl & IntNaCl) together with baselines under all attacks. From Figure S1, one can see that among all baselines, AdvW demonstrates the best adversarial robustness, whereas our proposals still consistently win over it by a noticeable margin.

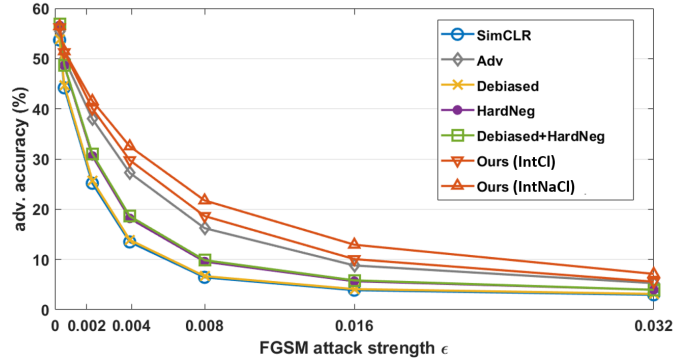
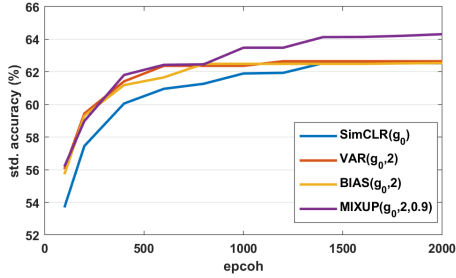


Figure S1: The adversarial accuracy under FGSM attacks of different strength on CIFAR100.

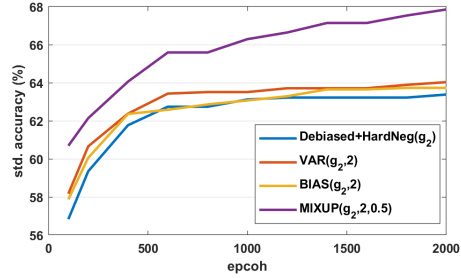
D Extended runtime

#epoch	100	200	400	600	800	1000	1200	1400	1600	1800	2000
$\mathcal{L}_{\text{SimCLR}}$	53.69	57.45	60.06	60.96	61.27	61.90	61.94	62.53	62.44	62.10	62.06
$\mathcal{L}_{\text{VAR}}(g_0, 2)$	56.04	59.44	61.42	62.37	62.06	62.36	62.65	62.47	62.43	62.45	62.15
$\mathcal{L}_{\text{BIAS}}(g_0, 2)$	55.72	59.31	61.19	61.66	62.49	61.95	62.06	62.39	62.39	62.52	62.54
$\mathcal{L}_{\text{MIXUP}}(g_0, 2, 0.9)$	56.20	58.98	61.81	62.43	62.46	63.48	63.48	64.13	64.14	64.21	64.31
$\mathcal{L}_{\text{Debiased+HardNeg}}$	56.83	59.35	61.77	62.74	62.68	63.12	63.22	63.08	62.86	62.90	63.38
$\mathcal{L}_{\text{VAR}}(g_2, 2)$	58.17	60.66	62.38	63.43	63.51	63.36	63.71	63.45	63.65	63.89	64.03
$\mathcal{L}_{\text{BIAS}}(g_2, 2)$	57.87	60.06	62.36	62.58	62.86	63.07	63.29	63.65	63.13	63.73	63.20
$\mathcal{L}_{\text{MIXUP}}(g_2, 2, 0.5)$	60.69	62.14	64.06	65.59	65.53	66.29	66.64	67.14	66.94	67.53	67.85

Table S5: The CIFAR100 linear evaluation results (%) after different numbers of training epochs.



(a) NaCl on SimCLR [4]



(b) NaCl on Debiased+HardNeg [13]

Figure S2: The standard accuracy (%) on CIFAR100 with extended runtime.

E Experimental details

Architecture. We follow [4, 13] to incorporate an MLP projection head during the contrastive learning on resnet18.

Optimizer. Adam optimizer with a learning rate of $3e - 4$.

Batching. A batch size of 256 is used across all the experiments.

Methodological hyperparameters. Throughout our experiments, we use $\tau^+ = 0.01$ and $\beta = 1.0$ for $\mathcal{L}_{\text{Debiased}}$ [5] and $\mathcal{L}_{\text{Debiased+HardNeg}}$ [13], $\alpha = 1$ for \mathcal{L}_{Adv} [14]. The same set of hyperparameters are used in our IntCl and IntNaCl.

Data augmentation. Our data augmentation includes random resized crop, random horizontal flip, random grayscale, and color jitter. Specifically, we implement the color jitter by calling `torchvision.transforms.ColorJitter(0.8 * s, 0.8 * s, 0.8 * s, 0.2 * s)` and execute with probability 0.8. Random grayscale is performed with probability 0.2.

Adversarial hyperparameters. When evaluating the adversarial robustness using the codebase provided in [40], we use a PGD step size of $1e - 2$, 10 iterations, and 2 random restarts.

Error bar. We run five independent trials for each of the experiments and report the mean and standard deviation for all tables and figures. The error bars in Figure S1 is omitted for better visual clarity.

F Supervised learning baseline

We give in the following the standard and adversarial accuracy of a supervised learning baseline with the same network architecture, optimizer, and batch size. In our self-supervised representation learning experiments, we train the representation network for 100 epochs and train the downstream fully-connected classifying layer for 1000 epochs. Therefore, to obtain a fair supervised learning baseline, we train the complete network end-to-end for 1000 epochs. We follow the same procedures in evaluating the transfer standard accuracy and adversarial accuracy as described in Section 5.

CIFAR100 (std. acc., FGSM acc., PGD acc.): 65.16 ± 0.32 , 35.89 ± 0.23 , 32.62 ± 0.23 .

Transfer CIFAR10 (std. acc., FGSM acc., PGD acc.): 77.45 ± 0.21 , 44.39 ± 0.47 , 40.35 ± 0.52 .